International Journal of Research in Engineering and Science (IJRES)
ISSN (Online): 2320-9364, ISSN (Print): 2320-9356
www.ijres.org Volume 09 Issue 11 ǁ 2021 ǁ PP. 66-70

Electric and Magnetic Properties of Synthesized Ni-Cu-Zn Ferrites

B. D. INGALE[1], R. M. MAHINDRAKAR[2], R. V. SURYAWANSHI[1]
[1]*Department Of Physics And Electronics, Azad Mahavidyalaya, Ausa, Dist- Latur-413520, M. S., India*
[2]*Department of Physics, Arts, Science And Commerce College Naldurga, Ta. Tuljapur, Dist. Osmanabad-413620, M. S., India*

ABSTRACT
Ferrites of composition [Ni $_{0.25-x}$ $Mg_xCu_{0.20}Zn_{0.55}$] Fe_2O_4 (x = 0.00, 0.05, 0.10, 0.15, 0.20 and 0.25) were prepared by the auto combustion method using citric acid as the fuel. XRD patterns showed the ferrites have a cubic spinel structure and lattice constant (a) decreases with increasing Mg^{2+} . A study of SEM images of the ferrites showed the permeability is correlated with the microstructures. DC resistivity and initial permeability were measured in the frequency range 100 Hz to 5 MHz. Permeability of the composition x = 0.15 observed as high due to densification and a low magnitostriction constant. The crystallite size was found to be 22.8 - 40.6 nm. The high permeability composition x = 0.15 has potential applications in multilayer chip inductors and surface mounting devices.
Key Words: *Ferrites, x-ray diffraction, permeability, optical parameters.*

Date of Submission: 12-11-2021 Date of acceptance: 28-11-2021

I. INTRODUCTION

Mg Cu Zn ferrites are the magnetic materials of choice for a wide range of applications because of their high permeability and environmental stability. The magnetostriction constant values of Mg Cu Zn materials are lower than those of Ni Cu Zn [1-6]. Mg-based ferrites are used in microwave devices because they have high electrical resistivity and low dielectric losses [7]. The substitution of diamagnetic ions of Mg^{2+} in spinel ferrites is known to produce changes in the electrical, magnetic and micro-structural properties [8-10]. Mg substitution in Ni Cu Zn ferrites improves the permeability and reduces the curie temperature [11]. It reduces the dielectric loss and decreases DC resistivity [12] .The grain size is better in Mg-substituted low-temperature sintered ferrites at higher frequency and low dielectric parameters [13]. For High-quality materials (Mg Cu Zn ferrite) with low losses at high frequencies Auto-combustion methods have been used. The properties of the Mg–Cu–Zn ferrites such as the permeability, nB values, magnetic moments from the hysteresis curve were determined using a VSM.

II. EXPERIMENTAL

Analytical grade magnesium nitrate [$Mg[N0_3]_2.6H_2O$], zinc nitrate [$Zn[NO_3]_2.6H_2O$], copper nitrate [$Cu\ [NO_3]_2.6H_2O$], iron nitrate [$Fe\ [NO_3]_2.9H_2O$] and citric acid [$C_6H_8O_7H_2O$] were used to prepare [$Ni_{0.25-x}\ M_x\ Cu_{0.20}\ Zn_{0.55}]Fe_2O_4$ with x=0.0, 0.05, 0.1, 0.15, 0.2 and 0.25 using the auto combustion method. The metallic nitrates and citric acid were dissolved in deionized water and mixed in a 1:3 M ratio of nitrate to citric acid. The solution was heated to transform it into a gel. The dried gel was burnt as in self propagating combustion until it was completely burned and formed loose powder calcined at 650^0C for 2 hours and it was granulated using PVA as a binder. It was uniaxially pressed with a pressure of 1.5-2 tons/cm^2 to form pellet and toroidal specimens. These specimens were sintered at 950° C for 4 hours. The crystallite sizes and lattice parameters of the sintered ferrites were determined through X-ray diffraction with CuKα radiation [λ=1.5406 Å]. The X-ray density was measured using the formula dx = ZM/Na^3. The bulk densities were measured using the liquid immersion technique. The bulk densities and porosities were calculated from the XRD data. Magnetic properties were studied using a VSM (model 4500 EG G Princeton Applied Research, USA) at 80 K. The DC resistivity was measured using the two-probe method. Dielectric measurements were carried out using an LCQR meter (HP-4284A) at 300 K in the frequency range from 100 Hz to 5 MHz. The inductance was measured using an LCQR meter to determine the permeability constant.

III. RESULTS AND DISCUSSION.

3.1 XRD Analysis

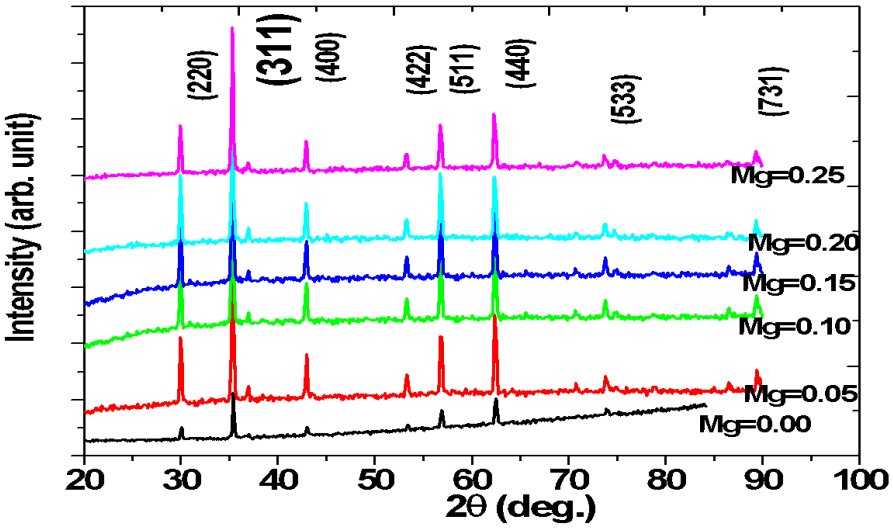

Figure 1. X-ray pattern of typical Mg substituted [Ni $_{0.25-x}$Mg $_x$Cu$_{.20}$ Zn$_{0.55}$]Fe$_2$O$_4$ ferrite

Fig. 1 shows the XRD pattern of a typical [Ni $_{0.25-x}$ Mg $_x$Cu$_{.20}$ Zn$_{0.55}$]Fe$_2$O$_4$ ferrite. The sintered ferrite has cubic spinel ferrite phases similar to that of JCPDS card No.33-0664. The broad peak XRD indicates that ferrite particles have small crystallite sizes. The lattice constant (a) slightly decreases with Mg substitution [8, 14]. When Mg^{2+} enters the crystal structure of the lattice the size of the unit cell decreases. Crystallite size of the ferrites ranged from 22.8 to 41.03 nm calculated using the Scherer formula. When burnt ashes of (Ni $_{0.25-x}$ Mg $_x$ Cu $_{0.20}$ Zn $_{0.55}$) Fe$_2$O$_4$ ferrite were sintered at 950°C for 4 hours, there was a noticeable effect on the crystallite size.

The crystallite size increased up to 0.15 with addition of Mg^{2+}.This may be attributed to the smaller ionic radius of Mg^{2+} (0.71)compared with that of Ni^{2+} (0.78) [16].The bulk density was found to increase with addition of Mg^{2+} composition.

The permeability increases with an increase in the Mg^{2+} content. It may be noted that the permeability values are correlated with the porosity contribution [9]. There is a sharp increase in the permeability of the composition at x = 0.15 may be mainly attributed to the decrease in the magnitostriction constant [16]. The initial permeability of the composition x = 0 is much lower than that of the composition x = 0.15, attributed to the lower bulk density, smaller crystal size and absence of Mg^{2+} in the composition [16]. The frequency dependency of the permeability in the present ferrites with different Mg^{2+} content[10, 11]. Increased frequency dispersion with Mg^{2+}content indicates the critical field decreases due to incorporation of Mg^{2+}. The permeability can be calculated from the inductance as

$$\frac{L}{0.0046\, N^2 h\, log_{10} \frac{d2}{d1}}$$

where L is the inductance ,
d1 is the inner and d2 is the outer diameter of toroid,
h is the height ,N is the number of turns
Permeability of x = 0.00 is lower than that of the composition x = 0.15. This may be attributed due to the lower grain size and the absence of Mg^{2+} in the present ferrites. Permeability is stable in the frequency range from 100 Hz to 1 MHz its dispersion occurs above 1 MHz. The high frequency dispersion is associated with domain wall dynamics. Increase in frequency dispersion upon incorporation of Mg^{2+} shows that the critical field decreases due to this incorporation [8, 10].

3.2 Study of Microstructure.

SEM images of specimens of x = 0.00, 0.05, 0.1, 0.15 and 0.2 are shown in Fig. 2. The samples sintered at 950°C for 4 hours have very dense microstructures with well-developed grains and few pores. These samples had small and homogeneous grains (average size 0.8342 µm) and pores, bulk density of the optimized sample was determined using the Archimedes method to be 6.99 g/cm^3.

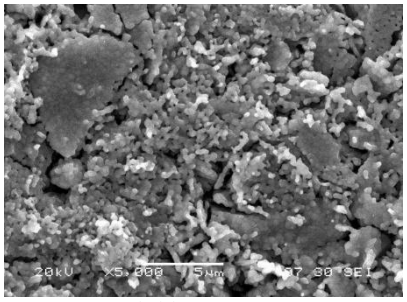

x = 0.00

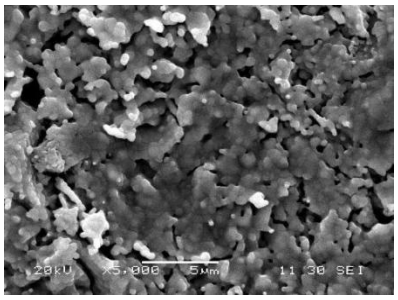

x = 0.05

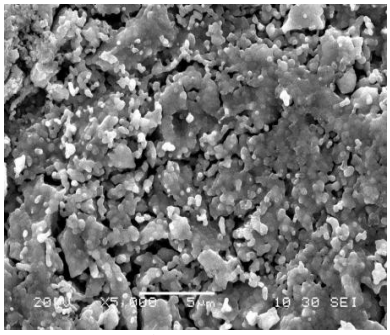

x = 0.15

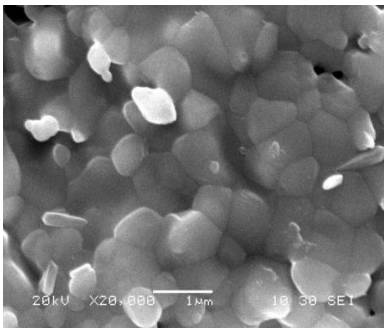

x = 0.20

Figure 2. SEM of x = 0.00, 0.05, 0.15 and 0.20

The perfectly spherical grains indicate that Ni-Co-Zi ferrite crystals were formed as confirmed by the XRD patterns. The grains and grain boundaries can be seen clearly. The grains are larger and the grain boundaries are broader, and there are intergranular pores[16].

3.3 Dc Resistivity

From Table 1 the resistivity decreases when Mg^{2+}content increases. The B sites of Mg^{2+} doped NiCuZn ferrites are occupied by Ni^{2+} Fe^{3+} and Cu^{2+} ions [16]. Obviously with a greater Fe^{2+} content conduction is better and consequently the resistivity is lower. The observed decrease in DC resistivity with increasing Mg^{2+} content may be attributed to the presence of more Fe^{2+} ions. The following equilibrium may exist during the sintering process:

$$Fe^{3+} + Mg^{2+} = Fe^{2+} + Mg^{3+} \qquad [12\text{-}15]$$

With increasing Mg^{2+} content, more Fe^{2+} is formed, resulting in an increased probability of electron hopping and reduced resistivity Table 1.

3.4 Magnetic Properties

Magnetic properties saturation magnetization (MS), retentivity (Mr) and coercive field (Hc) were studied by recording magnetic hysteresis loops using a VSM. The magnetic moment was calculated using the relation

$$nB = \frac{Mx\ Ms}{5585}$$

where Mx is the molecular weight of the ferrite sample, Ms is the observed saturation magnetization and 5585 is the magnetic factor. The VSM measurements were carried out at 80 K. The hysteresis loops of the $Ni_{0.25x}Mg_xCu_{0.20}Zn_{0.55}Fe_2O_4$ system are shown in Fig.3. The magnetic hysteresis loops of the samples indicate that the ferrite samples are magnetically soft with low coercivity and possess a ferromagnetic nature. The compositional data on the saturation magnetization (Ms), remanent magnetization (Mr) and Yafet–Kittel angle presented in Table 1. The decrease in Ms can be explained on the basis of the magnetic moment of Ni^{2+} (2.3 μB) and Mg^{2+} (1.1 μB) [16]. However, Mg^{2+} was partially distributed between the A-site and the B-site, while Zn^{2+} occupied the A-site strongly [16]. The values of the Bohr magneton (nB) were found to decrease with increasing Mg^{2+} content. This is because the A–B exchange interaction grew strong due to the replacement of Ni^{2+} ions by Mg^{2+} ions [16].

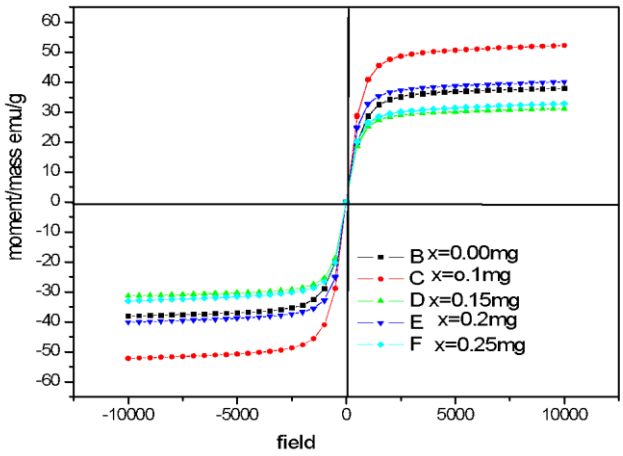

Figure 3. The hysteresis loops of the $Ni_{0.25x}Mg_xCu_{0.20}Zn_{0.55}Fe_2O_4$ series.

The decrease in M_S and nB is inferred from the Yafet–Kittel (*Y–K*) angle calculated from M_S and nB. With increasing Mg^{2+} content there is an increase in the angle $a_{Y\text{-}K}$. Hence there is additional canting at the sites A and B. The preferential occupation by Mg^{2+} ions of tetrahedral and octahedral sites in the ferrite sample results in the concentration of Fe^{3+} ions being reduced at these sites. The magnetic properties derive mainly from the highly magnetic Fe^{3+} ions present at the B-sites. The successive replacement of Fe^{3+} ions by Mg^{2+} ions decreases the Fe^{3+} Fe^{3+} (B–B) interaction. The coercivity field (HC) increases with increasing Mg^{2+} content for x = 0.15. A split sublattice molecular field model was developed by Yafet–Kittel. The Yafet–Kittel model was developed to explain the experimentally observed magnetic data of the Ni Zn system[17].

Table 1.

X content Mg.	Crystallite size from XRD(nm)	Grain size from SEM (μm)	D.C. Resistivity (Ω cm) at 100 kHz	Permeability (μ)	x-ray density	σs.emu/ gm	Ms.	nB	Cosαy-k
0.00	22.8	0.870	2.8×10^5	429	5.47	37.994	20.7827	0.889	$45^0 1' 19''$
0.05	38.81	0.797	3.3×10^3	290	5.29	52.224	27.624	1.173	$39^0 10' 17''$
0.1	39.28	0.797	3.1×10^3	372	5.26	57.476	30.232	1.275	$36^0 8' 2''$
0.15	**41.03**	**0.916**	**1.30×10^3**	**1177**	**5.22**	31.309	16.343	0.684	$48^0 2' 31''$
0.2	39.29	0.758	1.2×10^3	305	5.26	40.191	21.140	0.878	$43^0 23' 1''$
0.25	40.64	0.735	1.1×10^3	118	5.22	32.876	17.61	0.726	$47^0 1' 21''$

IV. CONCLUSIONS

1. XRD pattern indicates crystallite size and decrease in lattice constant with Mg^{2+}
2. Permeability increases up to x = 0.15.
3. The bulk density increases with addition of Mg^{2+}.
4. The values of (nB) decrease with increase in the Mg^{2+} .

REFERENCES

[1]. T. Nakamura, J. Magn.Magn.Mater.168 [1997] 285.
[2]. M.Fujimoto, J. Am Ceram.Soc. 77[11] 2873.
[3]. T. Ayoma. K. Hirota, O. yamguchi, J Am ceram.Soc.79 (10)(1996) 2792.
[4]. G.F. Dione R. G.west J.App.phys.81 (8) (1997) 4794.
[5]. S. F.wang. Y. R. Wang; Thomas C. K.yang; P. J.wang. C.A. Lu; J.Magn. Mater 217(2000).
[6]. Magn.Mater.251 [2002] 316-322Xi-Wei Qi, Ji Zhou, Zhenxing Yue, Zhi-Lun GUI. Long-Tu Li, J. Magn.
[7]. G. Ranga Mohan; D.Ravinder, A.V.Raman Reddy, B. S.Boyanov, Mater.Lett. 40 (1999) 39
[8]. M.I. Rosales, M.P. Cuautle, V. M. Castano, J, Mat. Sci-33 [1998] 3665.3669.
[9]. Effect of Mg substitution on Electromagnetic properties of $(Ni_{0.25-x} Mg_x Cu_{0.20} Zn_{0.55}) Fe_2O_4$ ferrite prepared by auto combustion method P. K. Roy, J. Bera, J. Magnetism magnetic material, 218(2006) 38-42.
[10]. Zhen-Xing Yue, Ji Zhou, Long – Tu Li, Xia ohui wang. Zhilum Gui,Mater. Sci. Eng. B 86[2OO1] 64-69.
[11]. Souilah Zahi [a,], Mansor Hashim [a], A.R. Daud, Materials Letters, 60(2006), 2803-2806.
[12]. M.A. ElHiti. J. Magn.Magn. Mater. 136 [1994] 138
[13]. B. Parvatheeswara Rao.K.H.Rao,J. Mater.Sci. 32[1997] 6049.
[14]. H.E. Scherrer, H. Kisker, H. Kronmuller, and R. Wurschum, Nanostruct. Mater. 6, 533 (1995).
[15]. D. M. Liu, j. M ater.Sci. 29 [1994] 1507.
[16]. S. M. Kabbur, U. R. Ghodake, Rahul C., Kambale S. D. Saratale, L. P. Chikhale and S. S. Suryawanshi, J. Electronic Material, DOI: 10.1007/s11664-017-5616-4, 2017, The minerals, Metals and Material Society.
[17]. Mahindrakar, R.M. (2017) Research Arena, ISSN 2320-6263, 4, Issue 10, 243-247